

# Heterogeneous Catalytic Oxidation of 5-hydroxymethylfurfural (5-HMF) To 2,5-Diformoylfuran (DFF) Using $\text{Fe}_3\text{O}_4@\text{C}$ Catalyst

Kalluri V.S Ranganath (✉ [ranganath.chem@bhu.ac.in](mailto:ranganath.chem@bhu.ac.in))

Banaras Hindu University Faculty of Science <https://orcid.org/0000-0001-9557-6747>

Rama Jaiswal

Banaras Hindu University Faculty of Science

---

## Research Article

**Keywords:** Magnetite, Oxidation of HMF, Heterogeneous Catalysis

**Posted Date:** May 6th, 2021

**DOI:** <https://doi.org/10.21203/rs.3.rs-492169/v1>

**License:**   This work is licensed under a Creative Commons Attribution 4.0 International License.

[Read Full License](#)

---

# Abstract

The selective oxidation of 5-hydroxymethyl furfural (HMF) to 2,5-diformylfuran (DFF) is one of the rapidly growing research area due to having its own importance in the fuel technology. We report a new heterogeneous catalyst for the oxidation of HMF to DFF in aqueous medium using a carbon soot deposited on magnetite ( $\text{Fe}_3\text{O}_4@\text{C}$ ). Further, the potentiality of our catalyst has also been realized in direct production of DFF from biomass (using either fructose or glucose) with high conversions via two consecutive steps.

## 1. Introduction

Due to rapid diminishing of fossil feedstock there is huge and enormous demand for sustainable and alternative feed stocks. Massive generation of biofuels from bio waste is one of the major challenging research areas to increase feedstock [1]. 5-hydroxymethylfurfural (5-HMF) is one of the molecules derived from the acid catalyzed dehydration of carbohydrates, which is having two functional groups (hydroxyl and aldehyde) and which is known for versatile application of liquid fuels [2]. The oxidation of 5-HMF leads to the formation of various value added products, out of which 2,5-diformylfuran (2,5-DFF) is one of the interesting compound for synthesis of pharmaceuticals, fungicides, heterocyclic ligands [3–4]. The selective oxidation of 5-HMF to 2,5-DFF is quite difficult due to the presence of highly reactive aldehyde [5]. In this direction, several researchers have reported the synthesis of DFF selectively from 5-HMF using a both homogeneous and heterogeneous catalysts. For instance, hydrotalcite supported ruthenium catalyst converted HMF to DFF in the presence of oxygen flow [6]. Further,  $\gamma\text{-Fe}_2\text{O}_3$  supported Ru/HAP [7]  $\text{V}_2\text{O}_5$  supported zeolite [8], Cu-MOR zeolites [9] have been reported in the direct oxidation of 5-HMF. In addition,  $\text{MnO}_2$  has been reported as a heterogeneous catalyst for the oxidation of 5-HMF to DFF in the presence of molecular oxygen or high air pressure [10] Therefore the development of highly efficient and cost effective catalytic protocol is highly desirable under the mild conditions.

Transformation of biomass-derived HMF to value-added platform chemicals such as DFF has been drastically increased during the past few decades due to having its own importance in fuel technology [11–17]. Oxidation of 5-HMF could produce many furan derivatives such as 2,5-diformylfuran (DFF), 2,5-furandicarboxylic acid (FDCA), 2,5-bis(hydroxyethyl)-furan (BHMF), 2,5-dimethylfuran (DMF) and clavulanic acid. Selective oxidation of 5-HMF that can be derived from biomass is of great importance for producing DFF as it can be used in the synthesis of several furan-containing functional polymers, poly-Schiff bases, pharmaceuticals, antifungal agents, and organic conductors [18]. In addition, the important application of DFF is in synthesis of macrocyclic ligands and also for a cross-linking agent for the synthesis of poly(vinyl-alcohol) [19–20]. HMF is one of the excellent chemicals for production of value-added furan derivatives owing to its unique structure which is a combination of highly reactive groups such as hydroxyl and aldehyde. These functional groups can also undergo different type of reaction such as hydrogenation, oxidation and hydrogen lysis of C-O bond [20]. Therefore, controlling the reaction condition for obtaining the selectivity towards DFF is remains a big challenge. Several heterogeneous

catalysts have been used for oxidation of HMF to DFF with high selectivity in the presence of oxidants like molecular oxygen and TEMPO in the presence of polar solvents like DMF and DMSO [21]. In addition, homogeneous catalysts have also been realized for the oxidation of HMF to DFF, however the major drawback of using homogeneous catalyst is difficult in its recovery and recyclability. Therefore, heterogeneous catalyst that can be recycled, are used for oxidation of HMF in the presence of various oxidants [22–33]. The concept of green synthesis is expected to integrate the DFF production in economically cheap solvent using the heterogeneous catalyst, which can be prepared by a simple method is having a lot of demand. Therefore, the development of a sustainable heterogeneous catalyst for the selective aerobic oxidation of HMF in the presence of a green solvent is still remaining challenged. Herein we report the development of  $\text{Fe}_3\text{O}_4@\text{C}$  a versatile and robust heterogeneous catalyst by a simple protocol using candle soot as a source of CNPs in the presence of iron chloride and polyvinyl alcohol. Thus, the developed  $\text{Fe}_3\text{O}_4@\text{C}$  has been used as an active potential candidate in the selective heterogeneous aerobic oxidation of 5-HMF in aqueous medium [34]. Here we have selected iron as supported materials due to its relatively non-toxic, abundant and possessing magnetic properties [35]. As carbon decorated metal oxides are used as an effective catalyst in various applications, promoted us to prepare CNPs on magnetite NPs [36–40]. Hence MNPs were selected to adsorb CNPs for the selective aerobic oxidation of 5-HMF. Thus the preparation process involves the deposition of carbon (from candle soot) on  $\text{FeCl}_3$  in the presence of polyvinyl alcohol. Thus, prepared catalyst is labelled as  $\text{Fe}_3\text{O}_4@\text{C}$ . Thus the synthesized material ( $\text{Fe}_3\text{O}_4@\text{C}$ ) has been well characterized using PXRD, SEM-EDX, Raman and XPS analysis (Scheme 1).

## 2. Experimental

**2.1** The aluminium plates and all chemicals were purchased from Sigma Aldrich. The aluminium plate were cut into square shaped disks (thickness = 1 mm, length = 20 mm). These disks were successively pre-treated by sonication using acetone, ethanol and Milli-Q water respectively. The  $\text{FeCl}_3$  in 5% PVA were allowed to stick on the aluminium plate. Later, candle (diameter = 10 mm) was lighted and metal salt coated aluminium plate near the tip of candle soot was placed. The soot was deposited from the tip of the flame on the disks in the presence of iron salts and kept it for 30 min. In this protocol, carbon particles deposited on iron oxide was removed (iron salt converted to iron oxide) from plate and washed with acetone and Milli-Q water and dried in oven at 120°C for 5 h.

### 2.2 Catalytic Application in the Oxidation of 5-HMF:

To an oven dried flask containing catalyst (5.0 mg), HMF (0.25 mmol) and base (2.0 equiv), the solvent (5.0 mL) were added and the reaction mixture was stirred at the required temperature. After completion of the reaction, (monitored by HPLC) catalyst was separated through centrifugation and washed with alcohol for further use. The conversion and selectivity's were calculated using HPLC.

## 3. Characterization

FT-IR analysis of heterogeneous catalyst was carried out using PerkinElmer Spectrum. Morphology of the resultant materials were characterized through XRD on an X-ray diffractometer equipped with a Cu K $\alpha$  radiation source ( $\lambda = 1.54$  nm). The chemical compositions were examined by EDX. The reaction was monitored by HPLC, using mobile phase: hexane: isopropanol (9:1) using C-18 column.

## 4. Results And Discussion

The catalysts have been characterized by using powdered X-ray diffraction (PXRD), to know the crystalline nature of the samples and its purity. The diffraction peaks of Fe<sub>3</sub>O<sub>4</sub>@C appeared at Bragg's angle at  $2\theta \sim 30.3, 35.3, 43.1, 53.1, 57.1, 62.7, 74.2$  corresponding to (220), (311), (400), (422), (511), (440) and (533) planes respectively. These data is attributed to Fe<sub>3</sub>O<sub>4</sub> face centred cubic structure [JCPDS card No. 89-0950]. In the XRD pattern of Fe<sub>3</sub>O<sub>4</sub>@C, no additional peaks were observed except the peak broadening, which is attributed to due to the presence of carbon on iron oxide (Fig. 1). The crystallite size was calculated by using Debye-Scherrer equation and found that 10.7 and 11.8 nm respectively for pure magnetite and Fe<sub>3</sub>O<sub>4</sub>@C respectively (Fig. 1).

Since Fe<sub>3</sub>O<sub>4</sub> has been successfully used in many oxidation reactions with good selectivity towards the desired product [41], initially the same catalyst has been evaluated in the aerobic oxidation of 5-HMF in the presence of various solvents. A variety of carbon materials including carbon nanotubes (CNTs), carbon nanofiber (CNF), graphene, graphene oxide (GO) and fullerenes have been extensively used in various biological and environmental applications [42-44]. Quite recently, carbon nanoparticles (CNPs) are being implemented for various applications due to their non-toxicity [45]. Synthesis of CNPs using candle soot is a simple technique, inexpensive and also another advantage is it take short period of time to synthesize [46-49]. In toluene, the oxidation of HMF has been carried out and observed that after 72 h very little conversion of HMF took place, either in the presence of a base or in the absence of a base at 100 °C (Table 1, Entry 1 & 2). However, in the presence of an oxidant like hydrogen peroxide 56% conversion of HMF was observed with 55.4% selectivity towards DFF in toluene using only Fe<sub>3</sub>O<sub>4</sub> as a catalyst (Table 1, Entry 3). There was no reaction either in the absence of base or absence of oxidant (Table 1, Entry 4). Remarkably, in the presence of base in aqueous medium, 58% conversion of HMF took place with 94.8% selectivity towards DFF. The other by products observed in this case are FDCA, FFCA and levulinic acid (Table 1, Entry 5). In the presence of hydrogen peroxide, though selectivity remains constant, but conversion increases to 74.8% using Fe<sub>3</sub>O<sub>4</sub> as a catalyst at 100°C whereas at 80°C, 68.4% conversion of 5-HMF was observed (Table 1, Entry 6 & 7). In the oxidation of 5-HMF, obviously (as expected) CNPs are quite inactive in aqueous medium in the presence of a base. To improve the catalytic activity, we incorporated CNPs inside magnetite and tested for the oxidation of HMF. It was found that in the absence of base, there was no oxidation of HMF took place using CNP/magnetite (Table 1, Entries 9-14). The rate of the reaction was triggered by the presence CNPs on magnetite. Notably, in the presence of oxidant like hydrogen peroxide, 93% conversion was observed after 72h using K<sub>2</sub>CO<sub>3</sub> as a base with 78.7% selectivity (Table 1, Entry 15). However, in the presence of oxygen (1.0 atm), using Fe<sub>3</sub>O<sub>4</sub>@C,

corresponding DFF product gave with 95.6% selectivity against 98% HMF conversion (Table 1, Entry 16). Temperature has a predominant effect on the conversion and selectivity in the oxidation of HMF.

Table 1  
Oxidation of 5-hydroxymethylfurfural to DFF using various solvents and catalysts

Entry	Catalyst	Base	Solvent	Oxidant	Temp. (°C)	Time (h)	HMF Conversion (%)	DFF Selectivity (%)
1	Fe <sub>3</sub> O <sub>4</sub>	-	Toluene	Air	100	72	< 10%	-
2	Fe <sub>3</sub> O <sub>4</sub>	K <sub>2</sub> CO <sub>3</sub>	Toluene	Air	100	72	< 10%	-
3	Fe <sub>3</sub> O <sub>4</sub>	K <sub>2</sub> CO <sub>3</sub>	Toluene	H <sub>2</sub> O <sub>2</sub>	100	72	56%	55.4%
4	Fe <sub>3</sub> O <sub>4</sub>	-	Water	Air	100	72	-	-
5	Fe <sub>3</sub> O <sub>4</sub>	K <sub>2</sub> CO <sub>3</sub>	Water	Air	100	72	58%	94.8%
6	Fe <sub>3</sub> O <sub>4</sub>	K <sub>2</sub> CO <sub>3</sub>	Water	H <sub>2</sub> O <sub>2</sub>	100	72	74.8%	95.4%
7	Fe <sub>3</sub> O <sub>4</sub>	K <sub>2</sub> CO <sub>3</sub>	Water	H <sub>2</sub> O <sub>2</sub>	80	72	86.4%	95.2%
8	CNPs	K <sub>2</sub> CO <sub>3</sub>	Water	Air	100	72	-	-
9	Fe <sub>3</sub> O <sub>4</sub> @C	-	Toluene	Air	100	12	< 1	< 1
10	Fe <sub>3</sub> O <sub>4</sub> @C	-	Toluene	Air	100	12	< 1	< 1
11	Fe <sub>3</sub> O <sub>4</sub> @C	-	water	Air	100	12	< 1	< 1
12	Fe <sub>3</sub> O <sub>4</sub> @C	-	DMF	Air	100	12	< 1	< 1
13	Fe <sub>3</sub> O <sub>4</sub> @C	-	DMSO	Air	100	12	< 1	< 1
14	Fe <sub>3</sub> O <sub>4</sub> @C	-	water	H <sub>2</sub> O <sub>2</sub>	100	12	< 1	< 1
15	Fe <sub>3</sub> O <sub>4</sub> @C	K <sub>2</sub> CO <sub>3</sub>	Water	H <sub>2</sub> O <sub>2</sub>	80	72	93	78.7
16	Fe <sub>3</sub> O <sub>4</sub> @C	K <sub>2</sub> CO <sub>3</sub>	Water	O <sub>2</sub>	80	72	98	95.6
17	Fe <sub>3</sub> O <sub>4</sub> @C	K <sub>2</sub> CO <sub>3</sub>	Water	H <sub>2</sub> O <sub>2</sub>	RT	72	35	11
18	Fe <sub>3</sub> O <sub>4</sub> @C	-	Acetonitrile	TEMPO	100	24	6	< 1
19	Fe <sub>3</sub> O <sub>4</sub> @C	K <sub>2</sub> CO <sub>3</sub>	Acetonitrile	TEMPO	100	72	63	74.6
20	Fe <sub>3</sub> O <sub>4</sub> @C	-	Water	TEMPO	80	72	< 1	< 1

Reaction Condition: substrate (0.25mmol), Catalyst (5.0 mg), Base (27.5mg), solvent (5.0 mL). Conversion and selectivity are calculated based on HPLC

Entry	Catalyst	Base	Solvent	Oxidant	Temp. (°C)	Time (h)	HMF Conversion (%)	DFF Selectivity (%)
21	Fe <sub>3</sub> O <sub>4</sub> @C	K <sub>2</sub> CO <sub>3</sub>	Water	TEMPO	80	72	95	95
Reaction Condition: substrate (0.25mmol), Catalyst (5.0 mg), Base (27.5mg), solvent (5.0 mL). Conversion and selectivity are calculated based on HPLC								

At room temperature, only 35% conversion took place with 11% selectivity (Table 1, Entry 17). In general oxidation of 5-HMF in low boiling aprotic solvent like acetonitrile gave the product in excellent yields with heterogeneous catalysts using TEMPO as an oxidant. In our case, we have also tested the potentiality of our catalyst in acetonitrile gave low conversion less than 6% along with other products FDCA, DFF and LA using TEMPO as an oxidant in the absence of a base and gave 63% conversion with 74.6% selectivity towards DFF in the presence of a base. (Table 1, Entry 18 and 19). Interestingly, in the presence of TEMPO as an oxidant using Fe<sub>3</sub>O<sub>4</sub>@C, conversion of 5-HMF has been observed 95% with 98% selectivity at 80 °C (Table 1, Entry 20 & 21). These results suggested that the introduction of CNP into metal oxide not only improve the catalytic activity, but also enhance the selectivity of DFF.

Notably, the reaction did not produce any product under catalyst free conditions. The candle soot supported iron salts confirms the Fe<sub>3</sub>O<sub>4</sub>@C hybrid as one of the best non-precious catalyst for the consecutive dehydration and oxidation reaction. The higher activity may be due to hydrophobic nature of carbon from the candle soot, resulted in a better Fe<sup>3+</sup> adsorption and enhanced dispensability. The higher activity of CNP/Fe<sub>3</sub>O<sub>4</sub> may be due to the facile redox reaction of Fe<sup>3+</sup> to Fe<sup>2+</sup> occurs in an easier way because of the synergetic effects of CNP on inverse spinel such as Fe<sub>3</sub>O<sub>4</sub> and thus reaction proceeds smooth way.

The heterogeneous catalyst Fe<sub>3</sub>O<sub>4</sub>@C has characterized by XPS, which confirms the presence of carbon incorporated on magnetite. (Fig. 1, SI). The doublet profile of Fe<sub>2p</sub> spectra into distinct Fe2p<sub>3/2</sub> and Fe2p<sub>1/2</sub> orbit at binding energies at 710.7 eV and 724.1 eV respectively. The stoichiometric magnetite Fe<sub>3</sub>O<sub>4</sub> of cubic close packed oxygen sublattice can be alternatively expressed as FeO•Fe<sub>2</sub>O<sub>3</sub>. Therefore, it consists of both iron ions Fe<sup>2+</sup> and Fe<sup>3+</sup> occupying the tetrahedral and octahedral interstices of cubic spinel type structure. The O 1s binding energy at 532.22 eV corresponds to O<sup>2-</sup> of Fe<sub>3</sub>O<sub>4</sub> showing only one kind of oxygen species. It was identified to be the bridge oxygen (O) between octahedral iron (Fe<sup>3+</sup>) and the tetrahedral (Fe<sup>2+</sup>) lattice. Further binding energy for C 1s was observed at 284.12 eV, 293.15 eV and 295.62 eV respectively, which is indicating the presence of different carbon species. The peaks at low binding energies nearly at 284 eV, are ascribed to the lattice carbon atoms, The binding energies corresponding to CNPs are 293 eV and at 296 eV, oxidized carbons, which may be present (Fig. 1, SI).

In addition, Fe<sub>3</sub>O<sub>4</sub>@C has also been characterized by Raman spectroscopy. It was employed to determine the nature of the iron oxide core (magnetite), where the Raman effect is caused by the molecular effects produced from certain energy irradiated on the sample. In the present case, the Raman spectrum peaks of iron oxide (Fe<sub>3</sub>O<sub>4</sub>) were investigated and found that translational movement (T<sub>2g</sub><sup>1</sup>) corresponding to FeO<sub>4</sub> are changed from 193 cm<sup>-1</sup> of Fe<sub>3</sub>O<sub>4</sub> to 214 cm<sup>-1</sup> for CNP/Fe<sub>3</sub>O<sub>4</sub> (Fig. 2). However, the asymmetric stretching (T<sub>2g</sub><sup>2</sup>) and bending of Fe-O (T<sub>2g</sub><sup>3</sup>) are remains same before and after incorporation of CNPs in the magnetite. Significantly, the symmetric bending of Fe-O of magnetite corresponding to E<sub>g</sub> has been shifted from 319 to 279 cm<sup>-1</sup> after incorporation of CNPs [50]. In addition, the peak at 680cm<sup>-1</sup> was identified as a band characteristic which was present on magnetite, however it has been disappeared in Fe<sub>3</sub>O<sub>4</sub>@C, which clearly indicates that hydrophobic CNPs have accommodated inside the magnetite, leads to the formation of crystal defects (Table 2).

Table 2  
Raman Shift Vibrations of Different Bondings in the on Fe<sub>3</sub>O<sub>4</sub> and CNP/Fe<sub>3</sub>O<sub>4</sub>

S.No	Vibrational Mode	Fe <sub>3</sub> O <sub>4</sub> (Cm <sup>-1</sup> )	Fe <sub>3</sub> O <sub>4</sub> @C (Cm <sup>-1</sup> )
1	T <sub>2g</sub> <sup>1</sup> (Translatory movement of FeO <sub>4</sub> )	193	214
2	T <sub>2g</sub> <sup>2</sup> (Asymmetric stretch of Fe-O)	488	485
3	T <sub>2g</sub> <sup>3</sup> (Asymmetric bend of Fe-O)	538	538
4	E <sub>g</sub> (Symmetric bend of Fe-O)	319	279
5	A <sub>1g</sub> (Symmetrical stretch of oxygen atoms along Fe-O)	683	670
6	Characteristic peak	1383	1286

Table 3  
Conversion of Biomass into DFF Catalyzed by CNP/Fe<sub>3</sub>O<sub>4</sub> Catalyst.

S.No	Substrate	Oxidant	HMF (%)	DFF (%) selectivity
1	Glucose	H <sub>2</sub> O <sub>2</sub>	-	99.3
2	Glucose	Air	-	84.3
3	Fructose	H <sub>2</sub> O <sub>2</sub>	< 1%	73.8
4	Fructose	Air	< 2%	94.8
Reaction condition: Substrate (1.0 mmol), Catalyst (5.0 mg), K <sub>2</sub> CO <sub>3</sub> (27.5mg), H <sub>2</sub> O (5.0 mL)				

The morphology and structural features of the Fe<sub>3</sub>O<sub>4</sub>@C has also been studied using scanning electron microscopy (SEM). Well defined spherical particles were observed with the nanometer size of approximately 20 nm and observed that all expected elements (Fe, O and C) are present on CNP/Fe<sub>3</sub>O<sub>4</sub> NPs (Fig. 3).

We have further investigated and potentiality of our catalyst in the one pot synthesis of DFF either from glucose or fructose [50–52]. In the case of glucose in the aqueous medium in the presence of air at 80°C, DFF was obtained with 99.3% selectivity and found that HMF has been completely converted. Remarkably, in the presence of air, it was also found that there was no HMF remained in the flask after 72 h and DFF was obtained with 84.3% selectivity. The other products formed under aqueous conditions are FDCA, FFCA and LA. Significantly, DFF has been obtained with 94.8% selectivity with complete conversion of fructose at 80°C with only 2% of HMF. This result clearly indicates that our developed catalyst CNP/Fe<sub>3</sub>O<sub>4</sub> could acts as a bifunctional catalyst where the subsequently dehydration and oxidation reactions took place. Of particular note is that no catalytic conversion of glucose or fructose was observed using magnetite alone.

In summary, we developed a new heterogeneous catalyst, operable under mild conditions, for the selective oxidation of HMF to DFF using candle soot derived, Fe<sub>3</sub>O<sub>4</sub>@C catalyst. Under optimized reaction conditions, we used water as a greener solvent using the robust heterogeneous catalyst. The present system circumvents the use of green protocols for utilizing biomass into value added products. The absence of precious metals and with the simple preparation of catalyst makes our catalytic protocol attractive not only for the selective oxidation of HMF to DFF, but also for the conversion of glucose/fructose. Our work will stimulate a lot of further research on the design of new heterogeneous catalysts for catalysis and the elucidation of the underlying modes of action.

## References

1. Zhang, J. Song, B. Haun, *Chem. Rev.* **117**, 6834-6880 (2017)
2. Zhou, Z. Xia, T. Huang, P. Yan, W. Xu, Z. Xu, J. Wang and Z. C. Zhang, *Green Chem.* **17**, 4206-4216 (2015)
3. Moreau, M. N. Belgacem, A. Gandini, *Top. Catal.* **27**, 11-30 (2004)
4. Rosatella, S. P. Simeonov, R. F. M. Frade and C. A. M. Afonso. *Green. Chem* **13** 754-793 (2011)
5. A. Halliday, R. J. Young, V. V. Grushin, *Org. Lett.* **11**, 2003-2005 (2003).
6. Mn-co binary oxide: Gui, S. Sarvanumurugan, W. Cao, L. Schill, L. Chen, Z. Qi, A. Riisager, *ChemistrySelect.* **2**, 6632-6639 (2017)
7. Biswas, B. Dutta, A. M.-Kannakithodi, R. Clarke, W. Song, R. Ramprasad, S. L. Suib, *Chem Comm* **53**, 11751-11754 (2017)
8. Nie, J. Xie, H. Liu, *J. Catal.* **301**, 83-91 (2013)
9. Tong, L. Yu, H. Chen, X. Zhuang, S. Liao, H. Cui, *Catal. Commun.* **90**, 91-94 (2017)

10. Ma, Z. Du, J. Xie, Q. Chu, Y. Pang, ChemSusChem. **4**, 51-54 (2011)
11. Neatu, N. Petrea, R. Petre, V. Somoghi, M. Florea, V. I. Parvulescu, Catal. Today. **278**, 66-73 (2016)
12. Ru/HAP: Z. Zhang, Z. Yuan, D. Tang, Y. Ren, K. Lv, B. Liu, ChemSusChem. **7**, 3496-3504 (2014)
13. Yang, W. Qi, R. Su, Z. He, Energy Fuels. **31**, 533-541 (2017)
14. Zhang, J. Xie, W. Hou, Y. Liu, Y. Zhou, J. Wang, ACS Appl. Mater. Interfaces, **8** 23122-23132 (2016)
15. Pal and S. Saravanamurugan, ChemSusChem **12**, 145-163 (2019)
16. Kong, Y. Zhu, Z. Fang, J. Kozinski, I. S. Butler, L. Xu, H. Song and X. Wei, Green Chem **20**, 3657-3682 (2018)
17. Xiang, X. Liu, P. Yi, M. Guo, Y. Chen, C. Wesdemiotis, J. Xu, and Yi. Pang, Polym. Int. **62**, 1517-1523 (2013)
18. -Shan Kong, X.-Long Li, H.-Jian Xu and Yao Fu, Fuel Processing Technology. **209**, 106528 (2020)
19. Liu, Z. Zhang, K. Lv, K. Deng and H. Duan, Appl. Catal A: General **472**, 64-71 (2014)
20. -Z. Yang, J. Deng, T. Pan, Q.-X. Guo, and Y. Fu, Green Chem **14**, 2986-2989 (2012)
21. Zhenzhen Yang, Wei Qi, Rongxin Su and Zhimin He, ACS Energy Fuels. **31**, 533-541 (2017)
22. Fang, R. Luque, Y. Li, Green. Chem. **18**, 3152-3157 (2016)
23. Yaun, B. Liu, P. Zhou, Z. Zhang, Q. Chi, Catal. Sci. Technol. **8**, 4430-4439 (2018)
24. Nie and H. Liu, J. Catal. **316**, 57-66 (2014)
25. Chen, Y. Guo, J. Chen, L. Song, and L. Chen, ChemCatChem. **6**, 3174-3181 (2014)
26. Carlini, P. Patrono, A.M.R. Galletti, G. Sbrana, and V. Zima, Appl. Catal. A: Gen. **289**, 197-204 (2005)
27. C. Navarro, A. C. Canos, and S. Chornet, Top. Catal. **52**, 304-314 (2009)
28. Sadaba, Y. Y. Gorbanev, S. Kegnaes, S. S. R. Putluru, R. W. Berg, and A. Riisager, ChemCatChem. **5**, 284-293 (2013)
29. -T Le, P. Lakshmanan, K. Cho, Y. Han and H. Kim, Appl Catal A: General. **464-465**, 305-312 (2013)
30. Nie, J. Xie, and H. Liu, J. Catal. **301**, 83-91 (2013)
31. Huynh, H. Savolainen, T. Vu-Duc, M. Guillemin and F. Iselin, Sci. Total Environ. **102**, 233-241 (1991)
32. For the review: Heterogeneous catalysis in water for DFF: M. Ventura, A. Dibenedetto and M. Aresta, Chim Acta, **470**, 11-21 (2018)
33. Iron based catalysts for biomass: H. Du, F. Deng, R. R. Kommalapati, A. S. Amarasekhara, Renewable Sustainable Energy Rev., **134**, 110292 (2020)
34. Fe<sub>3</sub>O<sub>4</sub>@C core shell NPs J Zheng, Z Q Liu, X S Zhao, M Liu, X Liu, and W Chu, **23**, 165601 (2012)
35. Li, S. Jiang, J. Haung, Y. Wang, S. Lu and C. Li, New. J. Chem. **44**, 478-486 (2020)
36. Jafari, K. Boustani and S. Farjami Shayesteh, J Supercond Nov Magn, **27**, 187-194 (2014)
37. Wang, Y. Yu, P.C. Chen, D.W. Zhang and C.H. Chen, Journal of Power Sources. **183**, 717-723 (2008)
38. Zhao, S. Wu, C. He, Z. Wang, C. Shi, E. Liu and J. Li, Carbon. **57**, 130-138 (2013)
39. Shaikh, M. Satanami and K.V.S. Ranganath, Cat. Commun. **54**, 91-93 (2014)

40. Arora, H. Kaur, R. Kumar, R. Kaur, D. Rana, C. S. Rayat, I. Kaur, S. K. Arora, P. Bubber and L. M. Bharadwaj, Carbon Nanostruct. **23**, 377- 382 (2015)
41. Cha, S. R. Shin, N. Annabi, M. R. Dokmeci, and A. Khademhosseini, ACS Nano. **7**, 2891-2897 (2013)
42. Kamran, Y.-J. Heo, J. W. Lee, and S. -J. Park, Micromachines, **10**, 234 (2019)
43. Park., M. Vosguerichian and Z. Bao, **Nanoscale**. **5**, 1727-1752 (2013)
44. Jariwala, V.K. Sangwan, L.J. Lauhon, T.J. Marks and M.C. Hersam, Chem. Soc. Rev. **42**, 2824-2860 (2013)
45. M. Abel, S. Pourmiri, G. Basina, V. Tzitzios, E. Devlin and G. C. Hadjipanayis, **Nanoscale Adv.** **1**, 4476-4480 (2019).
46. Liu, T. Ye, C. Mao Angew. Chem. Int. Ed., **46**, 6473-6475 (2007)
47. R. Mulay, A. Chauhan, S. Patel, V. Balakrishnan, A. Halder and R. Vaish, Carbon, **144**, 684-712 (2019)
48. Panta PC and Bergmann CP, J Material Sci Eng., **5**, 217 (2015)
49. Fructose to DFF: C. Laugel, B. Estrine, J. L. Bras, N. Hoffmann, S. Marinkovic, and J. Muzart, ChemCatChem **6**, 1195-1198 (2014)
50. Fructose to DFF: Z. -Z. Yang, J. Deng, T. Pan, Q. -X. Guo, Y. Fu, Green. Chem **14**, 2986-2989 (2012)
51. Glucose to DFF: X. Xiang, L. He, Y. Yang, B. Guo, D. Tong, C. Hu, Catal Lett **141** 735-741 (2011)
52. TEMPO for oxidation: N. Mittal, G. M. Nisola, L. B. Malihan, J. G. Seo, S-Poong Lee and W-Jin Chung, Korean J. Chem. Eng **31**, 1362-1367 (2014)

## Figures

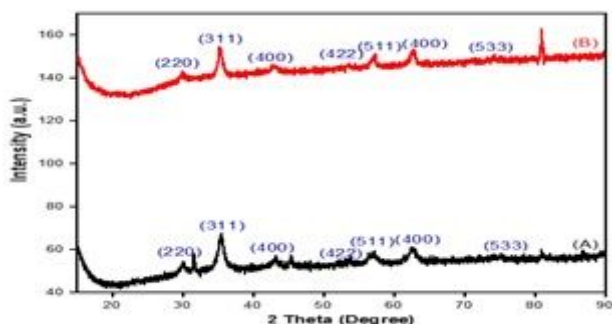


Figure 1

PXRD Pattern of (A) Fe<sub>3</sub>O<sub>4</sub> (B) Fe<sub>3</sub>O<sub>4</sub>@C

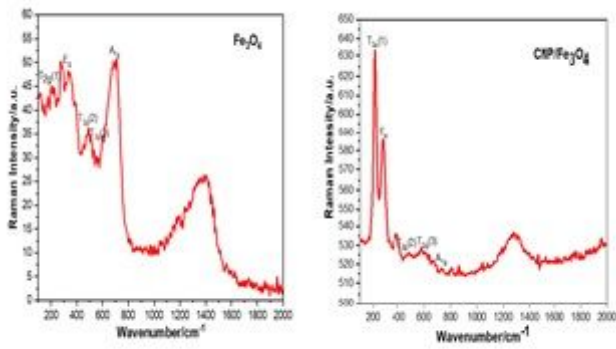


Figure 2

Raman spectra of Fe<sub>3</sub>O<sub>4</sub> and Fe<sub>3</sub>O<sub>4</sub>@C

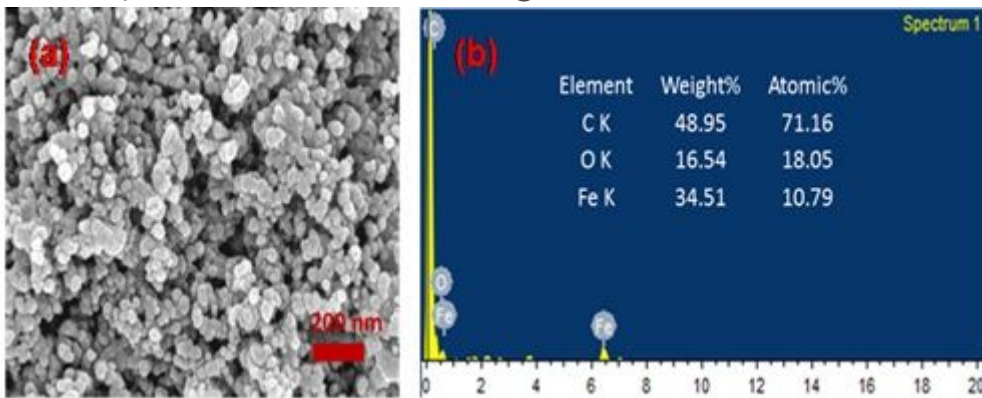


Figure 3

SEM-EDX analysis of CNP/Fe<sub>3</sub>O<sub>4</sub>

## Supplementary Files

This is a list of supplementary files associated with this preprint. Click to download.

- [SupportingInformationFinal.docx](#)